

Fig. 4. (A) FFP observed below the threshold current (6.7 A) by setting a fluorescent substance at a distance of 10 cm above the device. (B and C) FFPs observed above the threshold (6.9 and 7.4 A, respectively).

lattice PC, the frequencies of the four peaks shown in the inset of Fig. 2A can be used to determine the 2D optical coupling coefficients κ_1 , κ_2 , and κ_3 , which quantify the in-plane optical coupling effects for light waves propagating along the six equivalent Γ -X directions at 60° , 120° , and 180° to each other. Coefficients of $\kappa_1 \sim 830 \text{ cm}^{-1}$, $\kappa_2 \sim 510 \text{ cm}^{-1}$, and $\kappa_3 \sim 160 \text{ cm}^{-1}$, respectively, were obtained (10). Because the 2D band-edge effect is determined by the product of the coupling coefficients and the light-propagation length, we fixed the active PC area, where the current was injected, to $100 \times 100 \mu\text{m}^2$ in order to obtain sufficient band-edge effects.

We then measured the current–light-output power characteristics (10) of our device under the pulsed condition (a pulse width of 500 ns and a repetition rate of 1 kHz) at room temperature (Fig. 3A). A clear threshold characteristic at 6.7 A (equivalent to a current density of 67 kA/cm^2) was apparent. Figure 3B shows the emission spectra below and above the threshold. The spectra were measured by coupling the output light from the device to an optical fiber and then transferring it to a monochromator (10). Below the threshold current (6.5 A), the emission spectrum was broad, and four peaks were observed with a distribution similar to that shown in the inset of Fig. 2A. In contrast, the spectrum became sharp with a peak width of $\sim 0.15 \text{ nm}$ above the threshold (6.9 and 7.4 A), which was close to the resolution limit of the measurement system. The peak wavelength was 406.5 nm (in the blue-violet region). The emission peak above the threshold was much stronger than that below

the threshold, which is due to substantial improvement in the optical coupling between the output and the optical fiber (10). Finally, we measured the far-field pattern (FFP) below and above the threshold by placing a fluorescent substance at a distance of 10 cm above the device. Because of the need to insert a digital camera to record the FFP, it was not possible to align the fluorescent substance completely parallel to the device surface, which resulted in slightly asymmetric FFPs (Fig. 4). The FFP was broad below the threshold current (6.5 A) but was reduced to a small spot above the threshold (6.9 and 7.4 A). The beam divergence angle was as narrow as 1° , which indicated that large-area coherent lasing oscillation had been achieved, reflecting the characteristics of the PC-SEL.

At present, the laser operates with a large threshold current; however, the performance could be substantially improved by the following methods: (i) Improvement of the crystalline quality of the multiple-quantum-well active layer. Currently, the growth condition of the active layer on the 2D GaN/air PC formed by AROG process has not yet been optimized. Modification of growth conditions such as growth pressure and III-V ratio would improve the quality of the active layer. (ii) Optimization of the distance between the active layer and the PC. Currently, the distance is $\sim 150 \text{ nm}$, and the degree of mode overlap with the air holes is limited to $\sim 3.5\%$ (fig. S1) (10). If this distance were reduced to, for example, $\sim 60 \text{ nm}$, the band-edge effect could be increased, causing the threshold current to be substantially reduced. (iii) Use of a transparent

electrode. Currently, the top electrode is not transparent and thus blocks much of the surface emission. If a transparent electrode (or ring-type electrode) were used, the output power and/or efficiency could be improved.

References and Notes

1. M. Imada *et al.*, *Appl. Phys. Lett.* **75**, 316 (1999).
2. M. Meier *et al.*, *Appl. Phys. Lett.* **74**, 7 (1999).
3. S. Noda, M. Yokoyama, M. Imada, A. Chutinan, M. Mochizuki, *Science* **293**, 1123 (2001).
4. R. Colombelli *et al.*, *Science* **302**, 1374 (2003).
5. E. Miyai *et al.*, *Nature* **441**, 946 (2006).
6. R. Dorn, S. Quabis, G. Leuchs, *Phys. Rev. Lett.* **91**, 233901 (2003).
7. Y.-S. Choi *et al.*, *Appl. Phys. Lett.* **87**, 243101 (2005).
8. A. David *et al.*, *Appl. Phys. Lett.* **88**, 133514 (2006).
9. A. Usui, H. Sunakawa, A. Sakai, A. A. Yamaguchi, *Jpn. J. Appl. Phys.* **36**, L899 (1997).
10. See supporting material on Science Online.
11. K. Sakai *et al.*, *IEEE J. Selected Areas Commun.* **23**, 1335 (2005).
12. M. Imada, A. Chutinan, S. Noda, M. Mochizuki, *Phys. Rev. B* **65**, 195306 (2002).
13. K. Sakai, E. Miyai, S. Noda, *Appl. Phys. Lett.* **89**, 021101 (2006).
14. I. Vurgaftman, J. R. Meyer, *IEEE J. Quantum Electron.* **39**, 689 (2003).
15. This work was partly supported by a Grant-in-Aid and Global Center of Excellence (G-COE) program of the Ministry of Education, Culture, Sports, Science and Technology of Japan.

Supporting Online Material

www.sciencemag.org/cgi/content/full/1150413/DC1
SOM Text
Figs. S1 to S3
References

12 September 2007; accepted 21 November 2007
Published online 20 December 2007;
10.1126/science.1150413
Include this information when citing this paper.

Comparison of Comet 81P/Wild 2 Dust with Interplanetary Dust from Comets

Hope A. Ishii,^{1*†} John P. Bradley,^{1*} Zu Rong Dai,¹ Miaofang Chi,^{1,2} Anton T. Kearsley,³ Mark J. Burchell,⁴ Nigel D. Browning,^{1,2} Frank Molster⁵

The Stardust mission returned the first sample of a known outer solar system body, comet 81P/Wild 2, to Earth. The sample was expected to resemble chondritic porous interplanetary dust particles because many, and possibly all, such particles are derived from comets. Here, we report that the most abundant and most recognizable silicate materials in chondritic porous interplanetary dust particles appear to be absent from the returned sample, indicating that indigenous outer nebula material is probably rare in 81P/Wild 2. Instead, the sample resembles chondritic meteorites from the asteroid belt, composed mostly of inner solar nebula materials. This surprising finding emphasizes the petrogenetic continuum between comets and asteroids and elevates the astrophysical importance of stratospheric chondritic porous interplanetary dust particles as a precious source of the most cosmically primitive astromaterials.

The Stardust spacecraft collected thousands of comet dust particles measuring micrometers in size during its 6.1-km/s flight through the dusty coma and jets of comet 81P/Wild 2 (1–4). The dust was captured in optically clear, low-density, silica (SiO₂) aerogel and aluminum foils. Comet 81P/Wild 2 is believed to

originate in the Kuiper belt (1), a ring of icy objects extending from the orbit of Neptune at ~ 19 astronomical units (AU) out to $\sim 50 \text{ AU}$ (5). 81P/Wild 2 orbited between 5.0 and 19 AU with an ~ 40 -year period until perturbed by Jupiter's gravity in 1974 (6). The modified orbit provided a rare favorable opportunity for a low-relative-

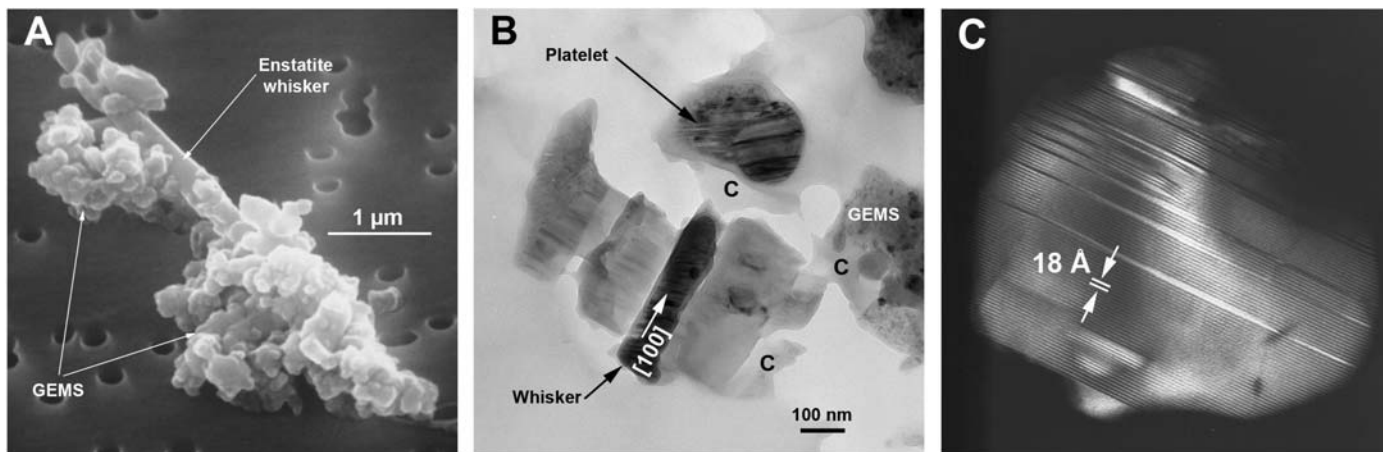


Fig. 1. CP IDP components. **(A)** Secondary electron image of CP IDP U25A30B mounted on a Nuclepore substrate. **(B)** Bright-field transmission electron micrograph of enstatite whiskers, platelets, GEMS, and carbonaceous material **(C)** in CP IDP U220A19. **(C)** Dark-field transmission electron micrograph of a <100-nm-thick enstatite platelet [systematics (h00) orientation] exhibiting 18 Å periodicity and numerous stacking defects in CP IDP CP16 α .

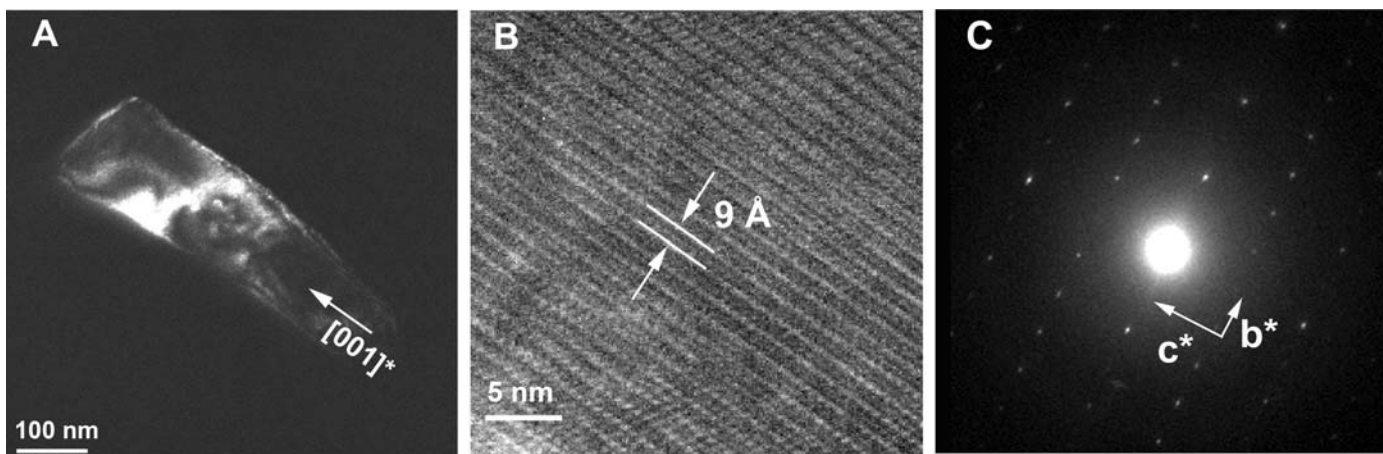


Fig. 2. Enstatite whisker in comet 81P/Wild 2 sample. **(A)** Dark-field transmission electron micrograph of a clino-enstatite whisker in Stardust track C2115,33,123,1,3 (Lucia). **(B)** Lattice-fringe image of the whisker showing 9 Å (010) lattice fringes. **(C)** [100] zone axis selected-area electron diffraction pattern.

velocity encounter. The comet experienced only five near-solar passes before the Stardust encounter, so solar processing of its surface was minimal, and 81P/Wild 2 has been widely anticipated to be a reservoir of presolar material, including stardust, cryogenically preserved since the accretion of the planets.

The returned sample was expected to include materials found in chondritic porous (CP) interplanetary dust particles (IDPs). Many IDPs entering Earth's atmosphere are from comets, and CP IDPs collected in the stratosphere by aircraft

exhibit properties consistent with cometary origin (7–9). Some CP IDPs are demonstrably cosmically primitive: Relative to other extraterrestrial materials, they are highly enriched in isotopically anomalous organic and inorganic outer solar nebula materials inherited, via the presolar molecular cloud, from the interstellar medium and circumstellar environments around other stars (10, 11). Although IDPs have been collected for ~40 years, the Stardust sample is a potential mother lode of presolar material from a known parent body containing 10^5 to 10^6 times the mass of an individual CP IDP and $\sim 10^3$ to 10^4 times the total mass of all CP IDPs examined to date.

Analysis of comet 81P/Wild 2 dust has revealed, in addition to silicates (olivines and pyroxenes) with a range of Mg to Fe ratios (4), refractory minerals formed in the inner nebula, probably within a few astronomical units of the early Sun. Minerals identified include melilite, anorthite, corundum, osbornite and roedderite associated as calcium-aluminum inclusions (CAIs), and probable chondrule fragments (4, 12). Refrac-

tory minerals, CAIs, chondrules, and chondrule fragments are normally absent from or exceedingly rare in CP IDPs but are found in almost all chondritic meteorites. Stardust has thus provided solid evidence of large-scale radial mixing in the solar nebula (1, 4), underscoring the importance of sample return missions.

CP IDPs contain two silicate materials believed to be unique to this class of meteoritic materials: amorphous silicates known as GEMS (glass with embedded metal and sulfides) that make up >50% by volume of most CP IDPs (8, 13), and exotic whisker and platelet morphologies of the crystalline silicate enstatite. Enstatite whiskers and/or platelets are present in all CP IDPs (14), constituting 1 to 5% by volume. A secondary electron image of a CP IDP (Fig. 1A) shows typical porous morphology (mostly GEMS) and an elongated enstatite crystal (a whisker). The typical petrographic setting of GEMS, enstatite whiskers, and platelets within CP IDPs is shown in a transmission electron micrograph from another CP IDP (Fig. 1B).

¹Institute of Geophysics and Planetary Physics, Lawrence Livermore National Laboratory, Livermore, CA 94550, USA.

²Department of Chemical Engineering and Materials Science, University of California Davis, Davis, CA 95616, USA.

³Department of Mineralogy, Natural History Museum, London SW7 5BD, UK. ⁴School of Physical Sciences, University of Kent, Canterbury, Kent CT2 7NH, UK. ⁵NWO (Netherlands Organization for Scientific Research), Anna van Saksestraat 51, Den Haag 2593 HW, Netherlands.

*These authors contributed equally to this work.

†To whom correspondence should be addressed. E-mail: hope.ishii@llnl.gov

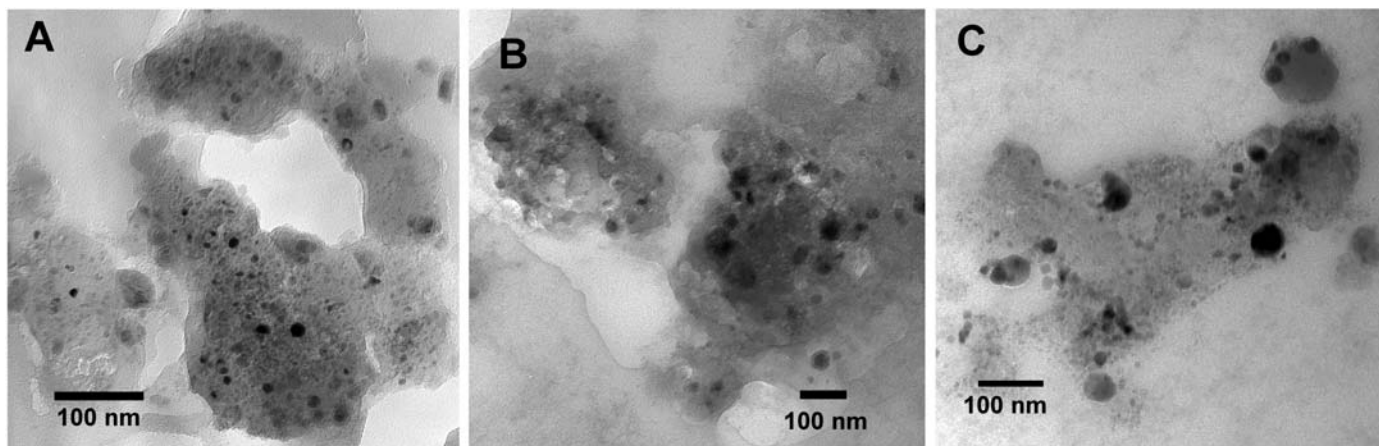


Fig. 3. GEMS and GEMS-like objects. Bright-field transmission electron micrographs of (A) GEMS in CP IDP U220A19, (B) GEMS-like material in Stardust track FC5,2,5,0, and (C) GEMS-like material produced by a light gas gun-generated hypervelocity impact of a pyrrhotite grain into aerogel at Stardust impact velocity.

Table 1. Bulk compositions of GEMS-like objects and GEMS. The mean, median, standard deviation, minimum, and maximum values of bulk compositions in atomic percent are given below for GEMS-like objects in Stardust tracks and GEMS in CP IDPs.

Atomic %	GEMS-like objects in Stardust ($n = 46$)					GEMS in CP IDPs ($n = 42$)				
	Mean	Median	SD.	Min.	Max.	Mean	Median	SD.	Min.	Max.
O	66.41	67.28	4.47	52.41	72.68	62.71	63.22	4.43	49.29	75.30
Mg	2.05	1.28	1.83	0.00	7.41	9.37	9.95	4.42	1.20	16.21
Al	1.42	1.20	1.27	0.00	5.92	1.62	1.29	1.09	0.25	5.90
Si	24.44	25.05	4.24	13.71	30.74	14.40	14.17	2.36	9.96	19.10
S	1.13	0.59	2.34	0.00	13.49	3.69	2.72	2.73	0.64	12.97
Ca	1.47	0.23	2.54	0.00	10.87	0.82	0.81	0.70	0.00	3.53
Cr	0.00	0.00	0.00	0.00	0.00	0.12	0.12	0.10	0.00	0.43
Mn	0.00	0.00	0.03	0.00	0.17	0.02	0.00	0.06	0.00	0.28
Fe	2.79	1.51	3.02	0.24	12.19	6.39	6.60	2.39	1.96	11.10
Ni	0.12	0.00	0.26	0.00	1.44	0.40	0.39	0.23	0.00	1.00

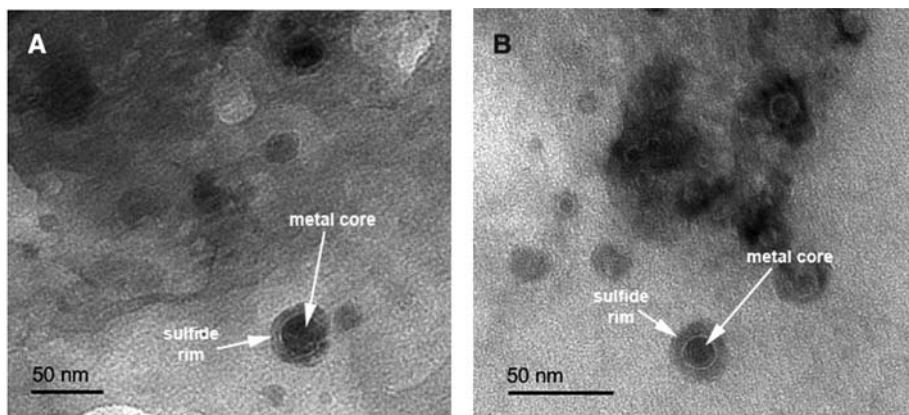


Fig. 4. Bright-field electron micrographs of sulfide grains after hypervelocity impact into aerogel at 6.1 km/s. (A) Stardust sample FC5,2,5,0,13 (Hopeful) shows sulfide rims on reduced metal cores. (B) Pyrrhotite laboratory shot fired at Stardust capture velocity into aerogel also results in sulfide rims on reduced metal cores.

Enstatite whiskers in CP IDPs are unique in that they are always elongated along the [100] crystallographic axis (14–16). In contrast, enstatite crystals in terrestrial rocks and meteorites, when not equiaxial, are elongated along [001]. Enstatite platelets in CP IDPs (15) include both ortho- and

clino-enstatite and are extremely thin along the [010] or [001] direction but not [100] (Fig. 1C). These enstatite whiskers and platelets probably condensed metastably above 1300 K from a low-pressure nebular gas (14). If 81P/Wild 2 accreted substantial quantities of outer nebula primitive

materials, then the Stardust sample should contain both GEMS and enstatite in whisker and platelet forms. Conversely, if 81P/Wild 2 contains mostly inner nebula materials as do the asteroid parent bodies of chondritic meteorites, then primitive material is rare in this comet, and from an astromaterials analysis standpoint, less-modified, larger quantities of Stardust-captured solids may be available in the existing meteorite collections. To explore these possibilities, we compared enstatite whiskers, GEMS, and GEMS-like materials in CP IDPs, Stardust samples, and laboratory samples using transmission electron microscopy (9).

A transmission electron micrograph (Fig. 2A) shows an elongated enstatite crystal in a Stardust impact track. Its morphology (Figs. 1B and 2A) and composition, almost pure MgSiO_3 with <0.5 weight % (wt %) Fe, are similar to those of enstatite whiskers in CP IDPs. Lattice-fringe imaging (Fig. 2B) and corresponding electron diffraction (Fig. 2C) establish that the crystal is monoclinic clino-enstatite. However, unlike whiskers in CP IDPs, this crystal is elongated along its [001]* axis. This is the only whiskerlike crystal we observed in the Stardust sample, although other enstatite crystals without whisker or platelet morphologies are present (4).

Typical GEMS in CP IDPs (Fig. 3A) are spheroids ~0.1 to 0.5 μm in diameter, composed of nanometer-sized inclusions of low-Ni α -iron (kamacite) and low-Ni iron sulfide (2C pyrrhotite) embedded in Mg-rich silicate glass (8, 13, 17). Some, and possibly all, GEMS are ancient (>4.6 billion years old) presolar interstellar amorphous silicates, a fundamental building material of solar systems (8, 9, 13, 18). GEMS-like material (Fig. 3B), abundant in some Stardust tracks particularly those containing sulfide particles, was initially interpreted as a promising link between 81P/Wild 2 and CP IDPs (3, 4). Like GEMS, it contains nanometer-sized inclusions of FeNi metal and sulfides embedded in glass. Unlike GEMS, the glass is

most often low-Mg silica (0 to 2 atomic % Mg), metal inclusions include both low-Ni α -iron and high-Ni γ -iron (taenite), sulfide inclusions often are partly reduced, and some sulfides contain Cu (4, 19). Table 1 shows that bulk compositions of GEMS-like material in Stardust tracks differ substantially from GEMS in CP IDPs (9). On average, the former has higher Si (by a factor of nearly 2) and lower Mg and Fe relative to the latter. A laboratory light gas gun shot (9) of micrometer-sized pyrrhotite particles into aerogel at 6 km/s resulted in abundant GEMS-like material (Fig. 3C) in each impact track above a remnant pyrrhotite particle. This material consists of nanometer-sized inclusions of metal and sulfides embedded in Mg-free silicate glass (compressed and melted aerogel). Like the Stardust GEMS-like material (Fig. 4A), many sulfide inclusions in this material produced by a laboratory-generated impact have reduced metal cores (Fig. 4B). This distinctive association demonstrates unequivocally that in Stardust tracks, GEMS-like material was created during capture by melting and intermixing of aerogel with crystalline minerals, including silicates and sulfides. These results emphasize the need for laboratory experiments (20, 21) to understand Stardust capture alteration of each component found in the 81P/Wild 2 sample.

Temperatures on impact were expected to reach several hundred kelvin (22) but exceeded 2000 K locally (1). Both Stardust and experimental tracks contain well-preserved sulfides and melted sulfides (~1000 K), decomposed and intermixed with melted aerogel, illustrating the compromised state of the Stardust sample and dramatic variation of thermal and shock conditions within single tracks due to capture (4). Given these conditions, we considered whether the GEMS-like material in Stardust tracks is cometary GEMS intermixed with aerogel. Simply diluting CP IDP GEMS with excess SiO₂ would preserve the original nonvolatile-element atomic ratios (excluding Si and O). Instead, Mg normalized by Al (Table 1), for example, is four times smaller in the GEMS-like material in Stardust. Even if there are cometary GEMS indigenous to 81P/Wild 2 in the Stardust sample, it may ultimately be impossible to unambiguously distinguish them because of their unfortunate similarity to impact-produced materials (Fig. 4). Because of their distinctive morphologies and ease of recognition, enstatite whiskers were the first crystalline silicates identified and described in detail in CP IDPs (15). Enstatite is a relatively robust mineral that has survived in abundance in Stardust tracks; however, no [100]*-elongated enstatite whiskers or platelets have yet been identified.

Additional CP IDP constituents under-represented in Stardust samples are carbonaceous material and presolar grains. Refractory carbonaceous material (Fig. 1B) is rare in Stardust tracks, with abundances more typical of chondritic meteorites (23), whereas CP IDPs are

the most carbon-rich meteoritic materials known, with 13 wt % C on average and as much as ~50% by volume (16, 24). Most refractory cometary carbonaceous material should have survived, given the survival of fully stoichiometric sulfides and partial reduction of others (Fig. 4A) (4, 19). Where organic material has been analyzed, D/H ratios lie well below values determined for CP IDPs (2). Grains of stardust identifiable by non-solar isotopic compositions are also rare. Only one presolar grain has been confirmed so far in the Stardust sample, compared to ~8 to 10 in single CP IDPs measured recently (2, 9, 11). The low abundances of carbon and isotope anomalies, the presence of a CAI and probable chondrule fragments, and the lack of GEMS and enstatite whiskers and platelets indicate that any petrologic relationship between 81P/Wild 2 and the parent bodies of CP IDPs is at best tentative.

The mineralogical and isotopic evidence to date suggests that comet 81P/Wild 2 more closely resembles an inner solar system asteroid than an outer solar system comet with primitive unaltered dust. Ongoing studies will clarify the relationship between 81P/Wild 2 and specific class(es) of asteroidal meteorites (25). Accumulating evidence suggests that the Kuiper belt is populated in part by objects that either accreted closer to the Sun and subsequently migrated outward or accreted in situ from transported inner solar nebula materials (26). The possibility of finding some refractory component of inner solar system CAIs and chondrules in a single comet nucleus was acknowledged even before the Stardust mission (27). The recent discovery of main-belt comets with asteroidal orbits and comae (28) indicates no clear demarcation in the early solar system between asteroid- and comet-forming regions. The distinction between comets and asteroids is, in many cases, simply a matter of aging (loss of volatiles) and orbital parameters (29).

The nondetection to date in comet 81P/Wild 2 samples of the most abundant and most recognizable silicate materials in cometary CP IDPs, combined with low abundances of carbon and presolar grains and the presence of characteristic inner solar system refractory materials, reinforces the scientific importance of stratospheric IDP collection. All captured 81P/Wild 2 particles were modified, many severely, during abrupt deceleration into aerogel and aluminum foil (1, 4). Stardust may also have collected a few contemporary interstellar dust particles from the Ulysses dust stream (1), but severe modification is expected for these as yet unrecovered particles, collected at about three times the 81P/Wild 2 capture speed. In contrast, the upper atmosphere has proven an ideal medium for gentle deceleration of small meteoritic particles traveling at cosmic velocities because of the gradual density gradient. CP IDPs are in continuous and inexhaustible supply, and many IDPs survive atmospheric entry with minimal thermal and shock alteration (8). At present, CP IDPs remain the most cosmically primitive astromaterials least

altered by capture that are currently available for laboratory study and a valuable resource for understanding the origins and evolution of planetary systems.

References and Notes

1. D. E. Brownlee *et al.*, *Science* **314**, 1711 (2006).
2. K. D. McKeegan *et al.*, *Science* **314**, 1724 (2006).
3. L. P. Keller *et al.*, *Science* **314**, 1728 (2006).
4. M. E. Zolensky *et al.*, *Science* **314**, 1735 (2006).
5. M. C. Festou, H. U. Keller, H. A. Weaver, Eds., *Comets II* (Univ. of Arizona Press, Tucson, AZ, 2004).
6. M. Królikowska, S. Szutowicz, *Astron. Astrophys.* **448**, 401 (2006).
7. D. E. Brownlee *et al.*, *Lunar Planet. Sci.* **XXVI**, 183 (1995).
8. J. P. Bradley, in *Treatise on Geochemistry*, A. M. Davis, H. D. Holland, K. K. Turekian, Eds. (Elsevier, London, 2003), vol. 1, pp. 689–711.
9. See supporting material on Science Online.
10. S. Messenger, *Nature* **404**, 968 (2000).
11. A. N. Nguyen, H. Buseman, L. R. Nittler, *Lunar Planet. Sci.* **XXXVIII**, 2332 (abstr.) (2007).
12. D. J. Joswiak, D. E. Brownlee, G. Matrajt, *Meteorit. Planet. Sci.* **42**, A78 (2007).
13. J. P. Bradley, *Science* **265**, 925 (1994).
14. J. P. Bradley, D. E. Brownlee, D. R. Veblen, *Nature* **301**, 473 (1983).
15. P. Fraundorf, *Lunar Planet. Sci.* **12**, 292 (1981).
16. L. P. Keller, S. Messenger, J. P. Bradley, *J. Geophys. Res.* **105**, 10397 (2000).
17. Z. R. Dai, J. P. Bradley, *Geochim. Cosmochim. Acta* **65**, 3601 (2001).
18. S. Messenger, L. P. Keller, F. J. Stadermann, R. M. Walker, E. Zinner, *Science* **300**, 105 (2003).
19. M. Chi *et al.*, *Lunar Planet. Sci.* **XXXVIII**, 2010 (abstr.) (2007).
20. A. T. Kearsley *et al.*, *Meteorit. Planet. Sci.* **42**, 191 (2007).
21. T. Noguchi *et al.*, *Meteorit. Planet. Sci.* **42**, 357 (2007).
22. D. E. Brownlee *et al.*, *Meteorit. Planet. Sci.* **35**, A35 (2000).
23. G. Matrajt *et al.*, *Meteorit. Planet. Sci.* **42**, A99 (2007).
24. L. P. Keller, K. L. Thomas, D. S. Mackay, in *Analysis of Interplanetary Dust*, M. E. Zolensky, T. L. Wilson, F. J. M. Rietmeijer, G. J. Flynn, Eds. (American Institute of Physics, New York, 1994), pp. 51–87.
25. M. Weisberg, *Eos* **87**, P51E-1243 (abstr.) (2006).
26. F. J. Ciesla, *Science* **318**, 613 (2007).
27. J. A. Wood, *NASA Conf. Pub.* **10152**, 61 (1989).
28. H. H. Hsieh, D. Jewitt, *Science* **312**, 561 (2006).
29. D. E. Brownlee, in *Treatise on Geochemistry*, A. M. Davis, H. D. Holland, K. K. Turekian, Eds. (Elsevier, London, 2003), vol. 1, pp. 663–688.
30. This work was funded in part by NASA Stardust Participating Scientist, Discovery Data Analysis, Sample Return Laboratory Instrument and Data Analysis, and Cosmochemistry programs (J.P.B. and H.A.I.). M.C. acknowledges a Lawrence Livermore National Laboratory (LLNL) Student Employee Graduate Research Fellowship. M.J.B. and A.T.K. thank NASA and the Jet Propulsion Laboratory/Caltech for Stardust aerogel and foil for laboratory experiments. Kent light gas gun work was supported by a Science and Technology Facilities Council grant. Portions of this work were performed under the auspices of the U.S. Department of Energy by LLNL under contract DE-AC52-07NA27344. Stardust track "Lucia" (C2115,33,123,0) was named in memory of Lucia Glen Molster (26 to 27 April 2007), the beloved daughter of Frank and Nathalie Molster.

Supporting Online Material

www.sciencemag.org/cgi/content/full/319/5862/447/DC1
Materials and Methods
SOM Text
References

18 September 2007; accepted 30 November 2007
10.1126/science.1150683

Comparison of Comet 81P/Wild 2 Dust with Interplanetary Dust from Comets

Hope A. Ishii, John P. Bradley, Zu Rong Dai, Miaofang Chi, Anton T. Kearsley, Mark J. Burchell, Nigel D. Browning and Frank Molster

Science **319** (5862), 447-450.
DOI: 10.1126/science.1150683

ARTICLE TOOLS

<http://science.sciencemag.org/content/319/5862/447>

SUPPLEMENTARY MATERIALS

<http://science.sciencemag.org/content/suppl/2008/03/20/319.5862.447.DC1>

RELATED CONTENT

<http://science.sciencemag.org/content/sci/319/5862/401.1.full>
[file:/contentpending:yes](http://science.sciencemag.org/content/sci/319/5862/401.1.full#file:/contentpending:yes)

REFERENCES

This article cites 26 articles, 8 of which you can access for free
<http://science.sciencemag.org/content/319/5862/447#BIBL>

PERMISSIONS

<http://www.sciencemag.org/help/reprints-and-permissions>

Use of this article is subject to the [Terms of Service](#)